HOKKAIDO UNIVERSITY

Title	Photoluminescence quenching in cobalt doped ZnO nanocrystals
Author(s)	Sekika Yamamoto
Citation	Journal of Applied Physics, 111(9), 094310 https://doi.org/10.1063/1.4710533
Issue Date	2012-05-07
Doc URL	https://hdl.handle.net/2115/49182
Type	journal article
File Information	ZnCoO2012JAP.pdf

Hokkaido University Collection of Scholarly and Academic Papers : HUSCAP

Photoluminescence quenching in cobalt doped ZnO nanocrystals

Sekika Yamamoto

Citation: J. Appl. Phys. **111**, 094310 (2012); doi: 10.1063/1.4710533
View online: http://dx.doi.org/10.1063/1.4710533
View Table of Contents: http://jap.aip.org/resource/1/JAPIAU/v111/i9
Published by the American Institute of Physics.

Related Articles

Enforced c-axis growth of ZnO epitaxial chemical vapor deposition films on a-plane sapphire
Appl. Phys. Lett. 100, 182101 (2012)

Photoluminescence induced by twinning interface in CdS nanocrystals
Appl. Phys. Lett. 100, 171911 (2012)

Effect of the doping level on the radiative life time in ZnO nanowires
J. Appl. Phys. 111, 084311 (2012)

Photoluminescence quenching processes by NO2 adsorption in ZnO nanostructured films
J. Appl. Phys. 111, 073520 (2012)

Tuning of mid-infrared emission of ternary PbSrTe/CdTe quantum dots
Appl. Phys. Lett. 100, 113112 (2012)

Additional information on J. Appl. Phys.

Journal Homepage: http://jap.aip.org/
Journal Information: http://jap.aip.org/about/about_the_journal
Top downloads: http://jap.aip.org/features/most_downloaded
Information for Authors: http://jap.aip.org/authors

ADVERTISEMENT

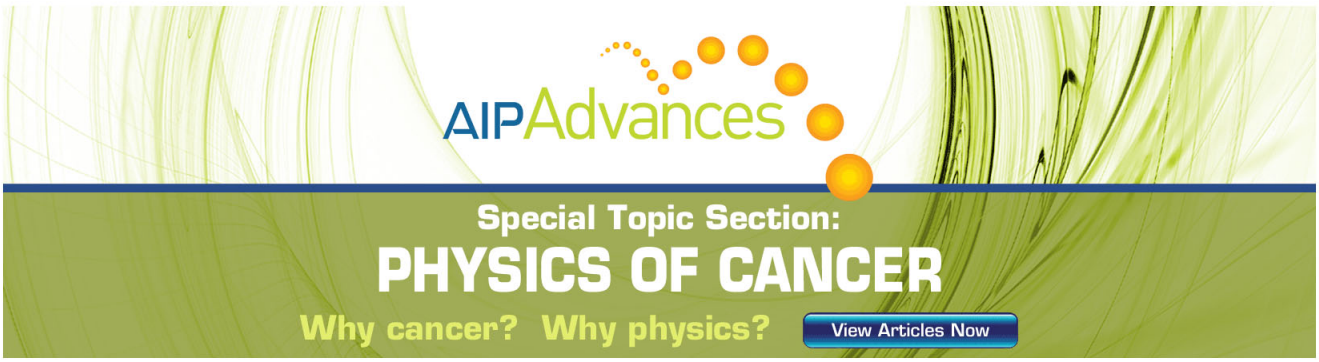

Photoluminescence quenching in cobalt doped ZnO nanocrystals

Sekika Yamamoto[a)]
Department of Physics, Graduate School of Science, Hokkaido University, N10W8, Sapporo 060-0810, Japan

(Received 3 February 2012; accepted 3 April 2012; published online 7 May 2012)

Influence of cobalt doping on the luminescence properties of ZnO nanocrystals with average diameter of 3.0 nm is investigated. Time resolved measurements at 20 K show that the dark exciton luminescence is completely lost in the nanocrystals doped with cobalt, while the perturbed luminescence with slight red shift survives and exhibits a non-exponential decay curve reflecting random distribution of cobalt atoms. By analyzing the non-exponentiality, the increase of the decay rate of the band-edge luminescence induced by the inclusion of single cobalt atom is estimated to be 0.012 ps^{-1}. © *2012 American Institute of Physics*. [http://dx.doi.org/10.1063/1.4710533]

I. INTRODUCTION

Semiconductor nanocrystals doped with transition metal ions possess remarkable optical and magnetic properties resulting from quantum confinement effect on carriers and exchange interaction between the carriers and the local spins of the metal atoms. These properties are expected to play an important role in future spintronic devices and currently being investigated rigorously. In the early stage of the research, doping of the nanocrystals is believed to be difficult due to self-purification effect.[1] However, recent investigation shows that the effect is not universal and differ material to material.[2] For example, Mn can be doped in InAs nanocrystal beyond the bulk solubility.[3]

Zinc oxide is a transparent material having a band gap energy of 3.37 eV at room temperature and thus capable of optical applications for whole visible light range. Preparing ZnO into a few nanometer size and doping it with metal atoms are expected to open a wide possibility for a variety of applications, which utilize their tunable optical and magnetic properties. Among the transition metals, divalent cobalt ion (Co[II]), which has an ionic radius of 0.56 Å, close to 0.60 Å of divalent zinc ion (Zn[II]), is known to be incorporated in ZnO nanocrystals up to 20%∼30% by substituting Zn site without destroying the wurtzite structure.[4,5] This makes ZnO:Co nanocrystal an ideal platform for investigating the optical and magnetic properties of the transition metal doped nanocrystal.

Besides many favorable properties mentioned above, the introduction of some kinds of metal ions into semiconducting materials has been known to cause significant drawbacks. The most important effect is the lifetime shortening of minority carriers, which leads to a strong quenching of the luminescence. It has been reported that 0.1% doping of Mn (Ref. 6) or 0.6% doping of Co (Ref. 7) into bulk ZnO crystal almost completely quench the luminescence, while the mechanism for these quenching has not been fully understood. In nanocrystal case, the quenching is more moderate compared with the bulk case. For example, it is reported that only 96% quenching is induced by 1.6% doping of Mn in ZnO nanocrystals of 6 nm size.[8] In another report, luminescence both from band-edge transition and from Co d-d transition are observed at the same time in ZnO:Co nanocrystals.[9]

In ZnO:Co case, it has been reported that the doped Co atom induces a charge transfer state just below the band gap energy.[10] The state can be detected by an enhancement of the light absorption around the band-tail region. This absorption also induces a photoconductivity by succeeding thermal excitation of the electrons to the conduction band.[11–13] It is believed that the optically generated electron-hole pair rapidly falls into this state from where it recombines non-radiatively by emitting phonons or by transferring its energy to cobalt d-multiplet,[14–16] but the details of this process are not clarified. We think that detailed understanding of the non-radiative process induced by the transition metal atoms is necessary for future application of these kinds of materials.

In this paper, we investigate the effect of Co doping on the luminescence properties of ZnO nanocrystals with strong quantum confinement and determine the quenching rate induced by the inclusion of single cobalt atom into the nanocrystal. The experimental results also imply that the quenching of the triplet luminescence is more efficient than that for the singlet luminescence and only one impurity in the nanocrystal causes a complete quenching of the luminescence.

II. EXPERIMENTAL

Zinc oxide nanocrystals are prepared as follows. First, 1.10 g of zinc acetate dehydrate ($ZnAc_2 \cdot 2H_2O$) is dissolved in 50 ml of absolute ethanol by boiling, and 0.29 g of lithium hydroxide monohydrate ($LiOH{\cdot}H_2O$) is dissolved in 50 ml of absolute ethanol ultrasonically. Typically, 10 ml of the Zn solution is heated to 70 °C before the same amount of LiOH solution cooled at 0 °C is poured under vigorous stirring. The solution is kept at room temperature for particle growth. After the desired particle size is attained, 200 mg of magnesium acetate tetrahydrate ($MgAc_2 \cdot 4H_2O$) is added into the solution and dissolved ultrasonically. The resulted solution is stored at room temperature at least for 3 days. After the addition of Mg salt, the particle growth is stopped and the suspension becomes very stable even at room temperature. No turbidity is recognized after one year storage at room temperature. The addition of Mg salt also leads to increased photoluminescence (PL) intensity. The details of the sample preparation are given

a)Electronic mail: sekika@mail.sci.hokudai.ac.jp.

 © 2012 American Institute of Physics

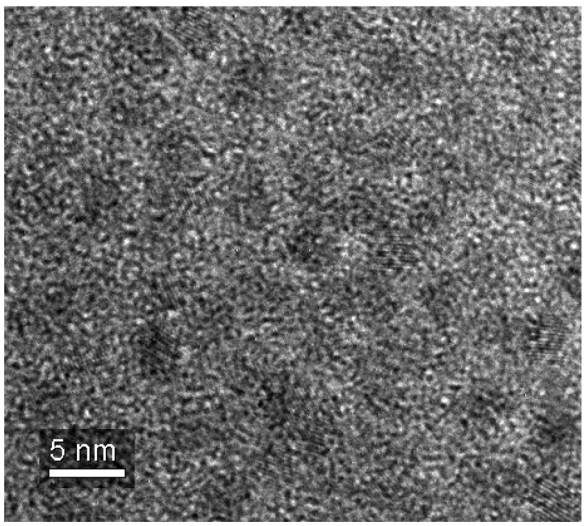

FIG. 1. A typical result of TEM measurements for undoped ZnO nanocrystals. The nanocrystals are almost spherical and their size is about 3 nm.

in the previous report.[17] For time resolved PL measurement, the third harmonics of a mode-locked Ti:Sapphire laser with a repetition rate of 80 MHz and a pulse duration of about 100 fs is used for the excitation source. Typical time averaged laser power density is 1 kW/cm^2. The detection of PL light is performed with a Hamamatsu C1587 streak camera system, which has a time resolution of about 20 ps.

III. RESULTS AND DISCUSSION

Figure 1 shows a typical result of TEM measurement for undoped nanocrystals. From the figure, it is estimated that the nanocrystals are almost spherical with their size about 3 nm. In Fig. 2, shown x-ray diffraction (XRD) results for (a) bulk ZnO (powder) and dried $Zn_{1-x}Co_xO$ nanocrystals with (b) $x = 0$ and (c) $x = 0.01$. The diffraction patterns for the nanocrystals clearly show that they have the same crystal structure with the bulk ZnO crystal and no extra signal for

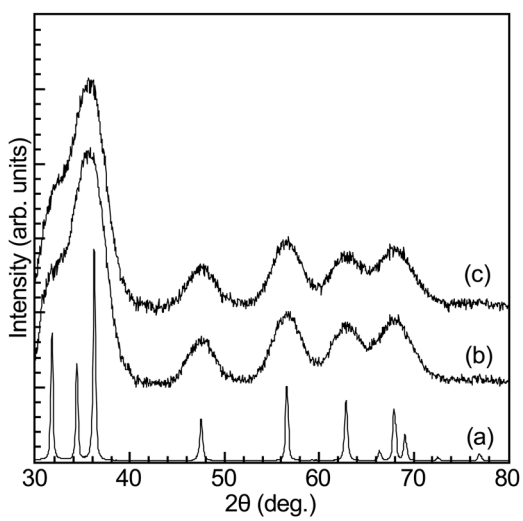

FIG. 2. XRD results for (a) bulk ZnO (powder) and $Zn_{1-x}Co_xO$ nanocrystals with (b) $x = 0$ and (c) $x = 0.01$. The analysis of the linewidth using modified Scherrer's formula gives 3.0 nm as an average diameters for the nanocrystals.

reaction byproducts such as zinc hydroxide[18,19] is recognized. The incorporation of Co does not seem to induce any change of the diffraction pattern although the minor changes such as small lattice expansion or small distortion cannot be distinguished because of the line broadening. The broadening reflects the smallness of the nanocrystals and we can estimate the average nanocrystal size from the linewidth by applying the modified Scherrer's formula.[20] The estimation gives a value of 3.0 nm as an average diameter of the nanocrystals, which is consistent with the TEM result.

Figure 3 shows absorption and PL spectra for $Zn_{1-x}Co_xO$ nanocrystals with $x = 0 \sim 0.01$ dispersed in ethanol. It is observed that the absorption edge is at higher energy than the bulk edge of 3.32 eV (Ref. 21) due to quantum confinement effect. The absorption edge further blue-shifts with increasing Co concentration. The dependence of the shift on the Co concentration x is estimated to be $3.8x$ eV. This is close to $3.56x$ eV (Ref. 13) or $2.6x$ eV (Refs. 15 and 16) observed in bulk ZnCoO. Therefore, we think that the shift mostly reflects the band-gap widening caused by the incorporation of the Co atoms. However, the larger blue-shift for the nanocrystals may indicate the smaller size of the doped nanocrystals. In this case, the size shrinkage of the doped nanocrystals can be estimated from the known size dependence of the band gap ($\Delta D/\Delta E \sim 2.83$ nm/eV around 3.7 eV) for ZnO nanocrystals,[22] and the estimation shows that the shrinkage should be less than 0.035 nm for $x = 0.01$ even when we consider the worst case of $2.6x$ for the bulk band gap shift on Co doping.

The inset of the Fig. 3(a) shows internal d-d absorption of the cobalt atoms. Absorption spectrum corresponding to the transition ${}^4A_1(F) \rightarrow {}^4T_1(P)$ with intensities almost proportional to the nominal doping level is clearly observed at the region 1.8~2.8 eV. The peak of the absorption is observed at 2.05 eV (605 nm) and it is indicative of internally doped Co(II) under T_d ligand configuration.[23,24] The externally attached atoms are known to exhibit the absorption peak at higher energy due to the modified ligand field.[24] We also see an enhancement of the absorption in the band-tail region between 3.0 and 3.6 eV. This absorption cannot be another d-d absorption because the intensity is much stronger. Instead, it is interpreted as a metal-to-ligand charge transfer absorption in which one of the d-electron of Co atom moves to the conduction band, or the valence band electron moves to cobalt d-states.[13] This absorption is also indicative of the internal doping.

In the PL spectra shown in Fig. 3(b), we observe two peaks of luminescence, one at 2.4 eV and the other at 3.65 eV. These two luminescence have been commonly observed in various ZnO materials. The former is called Green PL and usually regarded as a trap luminescence related to an oxygen vacancy although precise origin is still under debate. The latter is called band-edge PL and related to the electronic states extended in the nanocrystal volume. The slight red shift of the peak energy from the absorption peak implies that some kinds of perturbations such as a charged trap affect the luminescence. The linewidth measured at 20 K where the homogeneous line width is negligible is about 0.11 eV. This value, together with the size dependence of the band gap energy

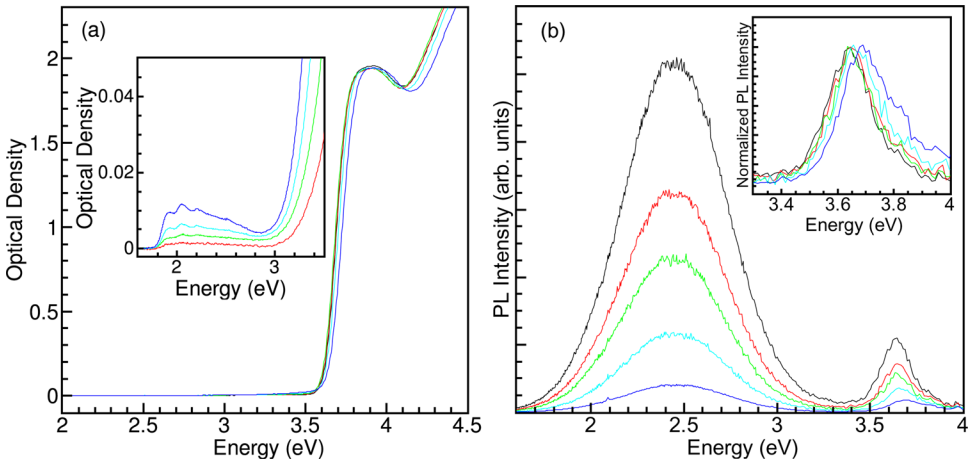

FIG. 3. Room temperature (a) absorption and (b) PL spectra for $Zn_{1-x}Co_xO$ nanocrystals with $x = 0$, 0.001, 0.002, 0.005, and 0.01 dispersed in ethanol. The absorption spectra are measured with a 1 mm thick optical cell. The inset in (a) shows absorption increase relative to the undoped sample measured in the mid-gap region. The inset in (b) shows normalized spectra of the band-edge PL. In all figures the cobalt concentration increases from black to blue.

shown above, implies that about 10% of size fluctuation exists in our sample.

As shown in the figure, the intensity for both peaks are greatly decreased when the Co impurity is incorporated into the nanocrystals. It is also seen in the figure that the band-edge PL shifts to higher energy with increasing Co doping. The shift for the sample with $x = 0.01$ is about 55 meV and it is larger than the shift of the absorption edge. This large shift may be understood if we take into account the size distribution of nanocrystals. It has been reported that the impurity atoms tend to be excluded from the nucleation of nanocrystals and they are mainly incorporated in the particle growth process.[23,24] Therefore, the smaller particles include fewer impurity atoms and the luminescence from the small particles should be relatively strong. The PL intensity from these particles will be emphasized when the impurity concentration is high. This explains the blue shift of the PL spectrum at high Co concentration.

Figure 4 shows results of time resolved measurements for the band-edge PL performed at 20 K using streak camera system. Figure 4(a) is for the undoped ZnO nanocrystals and Fig. 4(c) is for $x = 0.005$ sample. In the undoped sample, we see two components with different peak energies and different lifetimes. One is at 3.65 eV with shorter lifetime and the other at 3.73 eV with much longer lifetime. The latter has signal intensity also at the negative time region because the lifetime of this component is longer than the repetition period of the laser system (12.5 ns in this case) and the long tails from the previous pulse events are superposed in the measurement time window. The lifetime is estimated to be about 0.1 μs from the intensity of the superposed tail signal. The procedure of the lifetime estimation have been described in our previous report.[25] It was also shown from detailed temperature dependence that the Stokes shift for this component was very small and it must be interpreted as a dark exciton PL, which has a spin triplet nature and, therefore, a long radiative lifetime.[25] This effect is more prominent in nanocrystals because the quantum confinement effect enhances the exchange interaction between electron and hole.[26] As to the low energy component, a larger Stokes shift (lower luminescence energy) and a faster decay imply that this component is affected by a kind of extra charge situated at the surface or at an internal trap because these perturbations violate the spherical symmetry of the potential and induces the mixing of triplet and singlet states and enhances the oscillator strength.[27] The superposed tail of the high energy component is almost time-invariant within the time window, and it can be subtracted numerically from the signal. The low energy component obtained as a result of subtraction (not shown) exhibits rather symmetric Gaussian-like spectrum except for the initial 200 ps where a fast decay of the high energy component is observed (see below).

When Co atoms are doped in the nanocrystals, the PL intensity is significantly decreased as seen in Fig. 4(c). The effect of the Co doping is stronger for the high energy component because of its much longer radiative lifetime. In the sample with $x = 0.005$, the intensity of the high energy component decreases to 1.7% of the undoped sample, and it is no longer recognized in the figure due to the color quantization. As described above, a ZnO crystal doped with Co has a charge transfer state just below the band gap energy. The optically generated electron-hole pair is considered to fall into this state and recombine non-radiatively.[14–16] In addition, it can be derived from the Tanabe-Sugano diagram[28,29] that many doublet states of Co d-multiplet lie near the band gap energy of ZnO, which enable the triplet state of the electron hole pair to directly transfer its energy to the Co d-multiplet through the Dexter-type energy transfer mechanism without going through the charge transfer state.[30] From these considerations, we deduce that the remaining PL intensity for the high energy component comes only from the nanocrystals without any Co incorporation. To confirm this, we calculate the PL intensity from pure ZnO nanocrystals among the doped ones. The assumption we take is that the distribution of Co atoms in the nanocrystals approximately follow the Poisson distribution of

$$P(n, xN) = (xN)^n \frac{e^{-xN}}{n!}, \tag{1}$$

where n is the number of Co atoms in a nanocrystal, which has N cations, and x is Co mole fraction of the specimen. The PL intensity from the nanocrystals free from Co doping is proportional to $P(0, xN)$. Figure 4(f) shows the mole fraction x estimated by applying the Eq. (1) to the intensity of the high energy component relative to the undoped sample. The estimated mole fraction almost reproduces the nominal

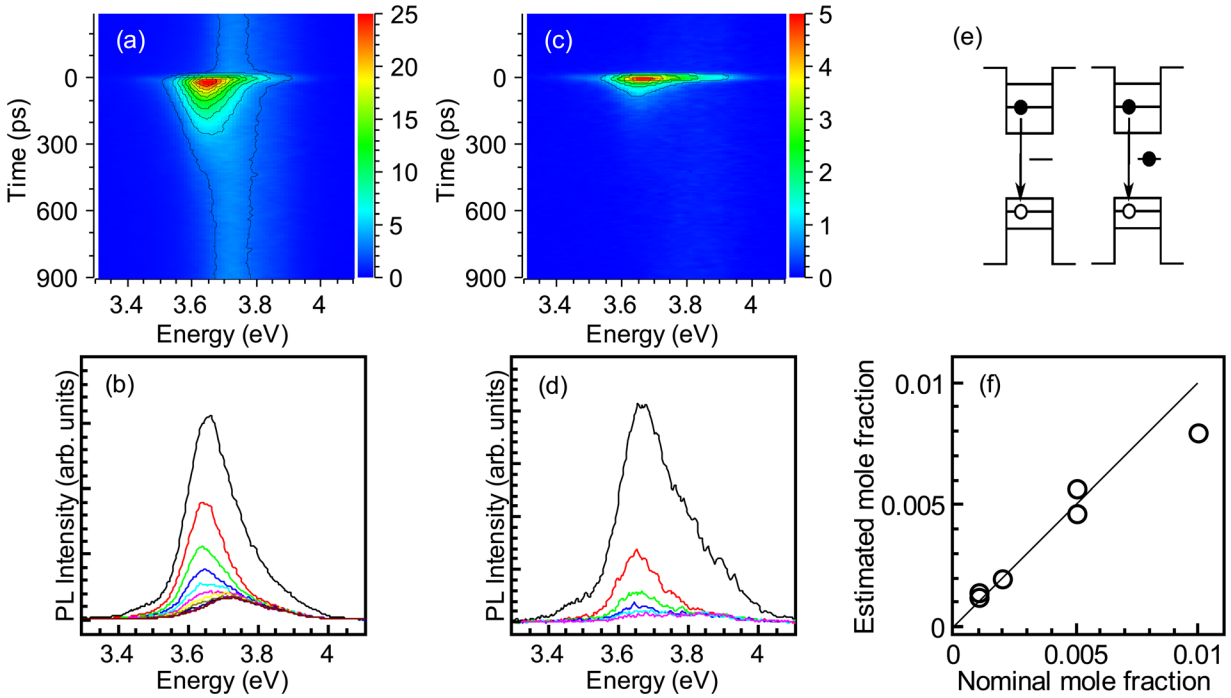

FIG. 4. Streak camera signal for (a) undoped and (c) $x = 0.005$ samples measured at $T = 20$ K. (b) and (d) are time resolved spectra extracted from the (a) and (c), respectively. The undoped sample shows a signal at negative time region because of its long lifetime longer than the laser repetition period. This component is interpreted as dark exciton PL and almost disappeared in the doped sample. The faster one seen at lower energy is a PL perturbed by a charge at the surface or internal trap state, which become faster in doped sample. (e) shows schematic diagram of the states. (f) shows mole fraction of cobalt atoms estimated under the assumption that the dark exciton PL comes only from the nanocrystals without any cobalt inclusion.

value and justifies the assumption. The slight deviation at $x = 0.01$ is probably due to the disregard of the particle size distribution. As mentioned above, very small particles are relatively difficult to dope and thus the existence of smaller particles enhances the PL intensity beyond the Poisson distribution, which leads to the underestimation of the mole fraction x.

Next, we evaluate the decay profile of each component by numerically decomposing the spectrum at every time slice into two components. Figure 5(a) shows an example of the decomposition. In the process, the spectrum at the negative time region is employed as the spectrum of the high energy component because the superposed tail signal does not include the low energy component. For the spectrum of the low energy component, a Gaussian shape is assumed. The peak energy and the width of the Gaussian are optimized in a preliminary fitting procedure and only the intensities of the two spectra are adjusted as fitting parameters in the main fitting procedure. The resulted decay profiles are shown in the Figures 5(b) and 5(c) for low and high energy components, respectively. From the analysis, it becomes clear that the high energy component consists of an initial fast decay before 200 ps and succeeding very slow decay, which makes up the superposed background. The initial fast decay is regarded as a transition from optically generated singlet state of the electron-hole pair to the optically inactive triplet state (dark exciton).[25] The inclusion of Co atoms into the nanocrystals makes the initial decay faster and the background weaker. This indicates that the non-radiative recombination caused by the Co atoms is faster than the triplet-singlet conversion.

As for the low energy component (Fig. 5(b)), the decay profile for undoped nanocrystals shows a single exponential decay reflecting the high quality of the sample. However, it becomes gradually non-exponential with increasing Co doping. We think that the non-exponentiality comes from the random distribution of the doped Co atoms in the nanocrystal. As shown above, the Co atoms are probably distributed randomly and the nanocrystals with higher number of Co atoms will show weaker and faster luminescence. So, we try to express the decay curves by the equation

$$I(t; x, \sigma_i) = I_0 \sum_n P(n, xN) \exp[-(\sigma_0 + n\sigma_i)t], \qquad (2)$$

where $\sigma_0 = 0.00775\ \mathrm{ps}^{-1}$ is the decay rate for the undoped nanocrystal, and σ_i is the enhancement of the decay rate per one inclusion of Co atom. We determine x and σ_i by fitting $I(t; x, \sigma_i)$ to the decay curves. The result of the fitting is shown by solid lines in the figure. The best fits are obtained for $\sigma_i = 0.012\ \mathrm{ps}^{-1}$. The result qualitatively reproduces the experimental decay curves and justifies the assumption of the random distribution of Co atoms. In addition, the estimated mole fraction x shown in Figure 5(d) qualitatively reproduces the nominal values of mole fraction. The deviation from the nominal value should be again caused by neglecting the particle size distribution that is manifested in the longer tail component beyond the fitting curves as most clearly recognized in the $x = 0.01$ sample.

The initial fast decay of the high energy component also becomes faster as Co doping is increased. It is difficult to evaluate the precise decay time of this component because it

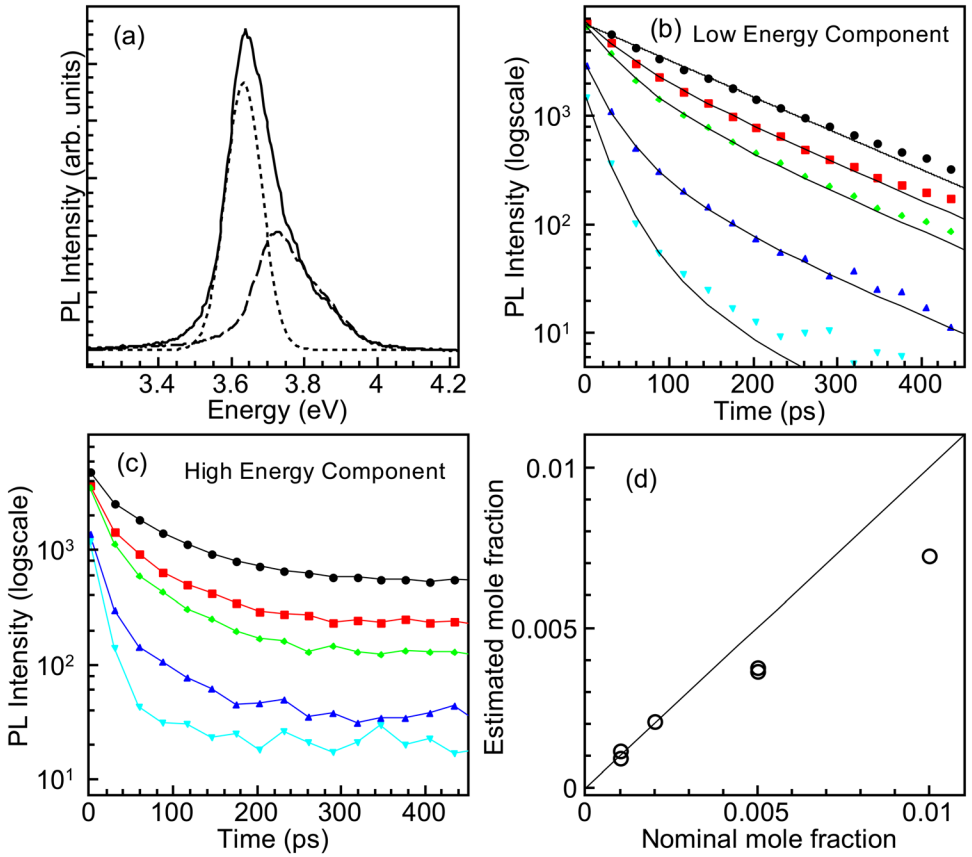

FIG. 5. Decay profiles for the two components of the band-edge PL evaluated by numerical decomposition of the time resolved spectrum. Figure (a) shows an example of the decomposition. (b) and (c) shows obtained decay profiles of the two components. (d) shows cobalt mole fractions estimated from the curve fitting of the decay profile for the low energy component under the assumption of Poisson distribution of cobalt atoms.

is comparable to the time resolution of our system. However, a rough estimate of the decay rate for $x = 0$ and $x = 0.01$ sample gives an enhancement of $\Delta\sigma \sim 0.06\ \mathrm{ps}^{-1}$ and dividing this value with average Co number per particle gives $\sigma_i' \sim 0.01\ \mathrm{ps}^{-1}$. This is comparable to the value σ_i for the low energy component. Therefore, the mechanism for the non-radiative recombination for these two luminescences may be alike.

IV. CONCLUSION

Time resolved measurements on the band-edge PL from Co-doped ZnO nanocrystals are performed at 20 K. The high energy component of the luminescence can be understood as the emission from undoped nanocrystals whose number is given by the Poisson distribution. The result shows that the triplet luminescence is completely quenched in the doped nanocrystal. The decay curve of the low energy component of the band-edge PL changes from single exponential to multi-exponential as doping level is increased. These decay curves are also reproduced by the calculation assuming the Poisson distribution of the Co atoms. The increase of the decay rate caused by one Co inclusion is estimated as 0.012 ps^{-1} for the ZnO nanocrystal with 3.0 nm diameter. The result presented here will be important for elucidation of the mechanism of non-radiative recombination of carriers in transition metal doped nanocrystals.

[1]A. L. Efros and M. Rosen, Annu. Rev. Mater. Sci. **30**, 475 (2000).
[2]S. C. Erwin, Phys. Rev. B **81**, 235433 (2010).
[3]C. A. Stowell, R. J. Wiacek, A. E. Saunders, and B. A. Korgel, Nano Lett. **3**, 1441 (2003).
[4]I. Bilecka, L. Luo, I. Djerdi, M. D. Rossel, M. Jagodič, Z. Jagličić, Y. Masubuchi, S. Kikkawa, and M. Niederberger, J. Phys. Chem. C **115**, 1484 (2011).
[5]R. Djenadic, G. Akgül, K. Attenkofer, and M. Winterer, J. Phys. Chem. C **114**, 9207 (2010).
[6]M. Liu, A. H. Kitai, and P. Mascher, J. Lumin. **54**, 35 (1992).
[7]D. Kouyate, J. C. Ronfard-Haret, P. Valat, J. Kossanyi, U. Mammel, and D. Oelkrug, J. Lumin. **46**, 329 (1990).
[8]N. S. Norberg, K. R. Kittilstved, J. E. Amonette, R. K. Kukkadapu, D. A. Schwartz, and D. R. Gamelin, J. Am. Chem. Soc. **126**, 9387 (2004).
[9]P. Lommens, P. F. Smet, C. M. Donega, A. Meijerink, L. Piraux, S. Michotte, S. Mátéfi-Tempfli, D. Poelman, and Z. Hens, J. Lumin. **118**, 245 (2006).
[10]K. R. Kittilstved, W. K. Liu, and D. R. Gamelin, Nature Mater. **5**, 291 (2006).
[11]W. K. Liu, G. M. Salley, and D. R. Gamelin, J. Phys. Chem. B **109**, 14486 (2005).
[12]S. A. Chambers, D. A. Schwartz, W. K. Liu, K. R. Kittilstved, and D. R. Gamelin, Appl. Phys. A **88**, 1 (2007).
[13]C. A. Johnson, A. Cohn, T. Kaspar, S. A. Chambers, G. M. Salley, and D. R. Gamelin, Phys. Rev. B **84**, 125203 (2011).
[14]R. Beaulac, P. I. Archer, and D. R. Gamelin, J. Solid State Chem. **181**, 1582 (2008).
[15]Z. Xiao, H. Matsui, N. Hasuike, H. Harima, and H. Tabata, J. Appl. Phys. **103**, 43504 (2008).
[16]Z. Xiao, H. Matsui, K. Katayama, K. Miyajima, T. Itoh, and H. Tabata, J. Appl. Phys. **108**, 13502 (2010).
[17]S. Yamamoto and T. Mishina, J. Lumin. **131**, 620 (2011).
[18]H. Zhou, H. Alves, D. M. Hofmann, W. Kriegseis, B. K. Meyer, G. Kaczmarczyk, and A. Hofmann, Appl. Phys. Lett. **80**, 210 (2002).
[19]P. Y. Wu, J. Pike, F. Zhang, and S. W. Chan, Int. J. Appl. Ceram. Technol. **3**, 272 (2006).
[20]A. L. Patterson, Phys. Rev. **56**, 978 (1939).
[21]J. F. Muth, R. M. Kolbas, A. K. Sharma, S. Oktyabrsky, and J. Narayan, J. Appl. Phys. **85**, 7884 (1999).
[22]E. A. Meulenkamp, J. Phys. Chem. B **102**, 5566 (1998).

[23]D. A. Schwartz, N. S. Norberg, Q. P. Nguyen, J. M. Parker, and D. R. Gamelin, J. Am. Chem. Soc. **125**, 13205 (2003).
[24]D. S. Bohle and C. J. Spina, J. Phys. Chem. C **114**, 18139 (2010).
[25]S. Yamamoto and T. Mishina, Phys. Rev. B **83**, 165435 (2011).
[26]A. L. Efros, M. Rosen, M. Kuno, M. Nirmal, D. J. Norris, and M. Bawendi, Phys. Rev. B **54**, 4843 (1996).
[27]S. Yamamoto, J. Phys. Chem. C **115**, 21635 (2011).
[28]Y. Tanabe and S. Sugano, J. Phys. Soc. Jpn. **9**, 766 (1954).
[29]F. A. Cotton, D. M. L. Goodgame, and M. Goodgame, J. Am. Chem. Soc. **83**, 4690 (1961).
[30]V. A. Vlaskin, N. Janssen, J. van Rijssel, R. Beaulac, and D. R. Gamelin, Nano Lett. **10**, 3670 (2010).